Title

Novel and robust treatment of pulmonary hypertension with netrin-1 and netrin-1-derived small peptides

Authors

Murugesan, Priya
Zhang, Yixuan
Youn, Ji Youn
et al.

Publication Date

2022-09-01

DOI

10.1016/j.redox.2022.102348

Peer reviewed

Redox Biology 55 (2022) 102348

Contents lists available at ScienceDirect

Redox Biology

journal homepage: www.elsevier.com/locate/redox

Novel and robust treatment of pulmonary hypertension with netrin-1 and netrin-1-derived small peptides

Priya Murugesan, Yixuan Zhang, Ji Youn Youn, Hua Cai *

Division of Molecular Medicine, Department of Anesthesiology, Division of Cardiology, Department of Medicine, David Geffen School of Medicine at University of California Los Angeles, United States

A R T I C L E I N F O

Keywords:
Pulmonary hypertension
Netrin-1
Netrin-1 derived small peptides
Hypoxia
Mean pulmonary arterial pressure (mPAP)
Right ventricular systolic pressure (RVSP)
Right ventricular hypertrophy
Pulmonary vascular remodeling
Nitric oxide (NO) bioavailability
Superoxide production
Endothelial nitric oxide synthase (eNOS) uncoupling
Oxidative stress

A B S T R A C T

Limited medical therapies have been implemented for the treatment of the devastating cardiorespiratory disease of pulmonary hypertension (PH) while none of which is sufficiently effective to stop or regress development of PH. We have previously shown that netrin-1, an axon-guiding protein during development, protects against ischemia reperfusion injury induced myocardial infarction via modest and stable production of nitric oxide (NO) and attenuation of oxidative stress. Since NO deficiency and oxidative stress-mediated vascular remodeling play important roles in the pathogenesis of PH, our present study investigated therapeutic effects on PH of netrin-1 and its derived small peptides. Infused into mice for 3 weeks during exposure to hypoxia, netrin-1 and netrin-1 derived small peptides V1, V2 or V3 substantially alleviated pathophysiological and molecular features of PH, as indicated by abrogated increases in mean pulmonary artery pressure (mPAP) and right ventricular systolic pressure (RVSP), attenuated right ventricular hypertrophy, diminished vascular remodeling of medial thickening and upregulation in smooth muscle alpha-actin (SMA) and proliferative cell nuclear antigen (PCNA), and alleviated perivascular and peribronchial fibrosis reflected by collagen deposition. NO bioavailability was substantially improved by treatment with netrin-1 and netrin-1 derived small peptides, while hypoxia induced increases in total superoxide production and eNOS uncoupling activity were all attenuated. These dual mechanisms of increasing NO bioavailability and decreasing oxidative stress at the same time, underlie robust protective effects on PH of netrin-1 and its derived small peptides, which are different from existing medications that primarily target NO signaling alone. Our data for the first time demonstrate intriguing findings that netrin-1 and netrin-1 derived small peptides can be used as novel and robust therapeutics for the treatment of PH.

1. Introduction

Pulmonary hypertension (PH) is a devastating, progressive disease of the pulmonary vasculature characterized by abnormally high mean pulmonary arterial pressure (mPAP) and right heart failure [1–3]. One of the major features of the disease is remodeling of the small blood vessels in the lung, and the resulting increase in vascular resistance [4–6]. The vascular alterations include smooth muscle cell proliferation with medial hypertrophy, arteriolar muscularization, fibrosis, *in situ* thrombosis and endothelial cell proliferation with subsequent intimal thickening. An array of vascular lesions form in human PH to result in progression of the disease, persistent increase in mPAP and eventually right heart failure. The pulmonary arterial endothelial cell dysfunction has been recognized as the primary event causing PH that is accompanied by impaired signaling in eNOS/NO [7,8].

Nitric oxide (NO) is a potent vasodilator that works by activating soluble guanylate cyclase (sGC) in vascular smooth muscle cells (SMCs) to catalyze the conversion of guanosine triphosphate (GTP) to cyclic guanosine monophosphate (cGMP), which results in vasodilation via protein kinase G (PKG). eNOS-mediated biosynthesis of NO in endothelial cells is considered the major source of bioavailable NO in the pulmonary circulation [9]. NO deficiency leads to endothelial dysfunction and development of PH. Therapies that target NO signaling such as inhaled NO, phosphodiesterase-5 (PDE-5) inhibitors (sildenafil and tadalafil) and sGC simulator (riociguat) have been shown to effectively relieve symptoms of PH [7,8,10], although these therapies have yet proven to stop or regress development of PH. One of the reasons for limited efficacies of these treatments might be related to the fact that these therapies do not necessarily attenuate oxidative stress (see below). In the present study, we demonstrated novel and robust therapeutic

* Corresponding author.
E-mail address: hcai@mednet.ucla.edu (H. Cai).

https://doi.org/10.1016/j.redox.2022.102348
Received 18 April 2022; Received in revised form 11 May 2022; Accepted 18 May 2022
Available online 26 May 2022

effects on PH of netrin-1 and netrin-1 derived small peptides, which are attributed to dual mechanisms of increasing NO bioavailability while alleviating oxidative stress. These mechanistic insights underlie maximal protective effects of netrin-1 and netrin-1 derived small peptides in substantially abrogating PH phenotypes at pathophysiological and molecular levels in the classical model of hypoxia induced PH.

The pulmonary vasculature undergoes morphological changes in PH that are mediated by oxidative stress [11]. Previous studies have documented changes in various oxidative stress markers in the lungs and pulmonary vasculature of animals and humans with PH [12,13]. Oxidative stress occurs when there are repeated external insults that provoke excessive ROS formation, which overwhelms antioxidant systems, thus creating an imbalance in the redox state of the cell favoring oxidation. Excessive synthesis of ROS can lead to cell and tissue damage due to oxidation of a number of cell constituents such as proteins, lipids, carbohydrates, and DNA. Oxidative stress has been implicated in the pathogenesis of a diversity of cardiorespiratory diseases such as atherosclerosis, diabetic vascular dysfunction, cardiac ischemia-reperfusion injury/myocardial infarction, and pulmonary and systemic hypertension [14–33]. We have previously shown that netrin-1, originally discovered as an axon-guiding molecule, exerts potent angiogenic and cardioprotective effects via production of NO upon DCC/ERK1/2 dependent activation of coupled eNOS, as well as inhibition of NADPH oxidase isoform 4 (NOX4) to alleviate oxidative stress, eNOS uncoupling activity, and mitochondrial dysfunction [23,27–29,31,34,35]. We have also shown that netrin-1 derived small peptides of 9–11 amino acids in length are able to provoke similar cardioprotective effects as exerted by full-length netrin-1 protein [31]. Indeed, we have confirmed that netrin-1 derived small peptides contain the core sequences to effectively bind to netrin-1 receptor DCC as the full-length netrin-1 protein does, to result in activation of ERK1/2/eNOS pathway to produce NO, while attenuating oxidative stress [23,27–29,31,34,35]. We hypothesized that these parallel mechanisms of NO stimulation and oxidative stress attenuation could mediate potential therapeutic effects on PH of netrin-1 and netrin-1 derived small peptides.

Therefore, in the present study, we investigated potential protective effects of netrin-1 and netrin-1 derived small peptides on PH in the classical model of hypoxia exposed mice. Through hemodynamic analyses, we found that netrin-1 and netrin-1 derived small peptides substantially or near completely alleviated hypoxia induced increases in mPAP and RVSP, as well as right heart hypertrophy. All of the pathophysiological and molecular features of PH including vascular remodeling of pulmonary arterioles characterized by medial thickness and increased expression in smooth muscle alpha actin (SMA) and proliferating cell nuclear antigen (PCNA), elevated ROS production, diminished NO bioavailability and increased eNOS uncoupling activity, were all substantially attenuated by netrin-1 and netrin-1 derived small peptides. Thus, netrin-1 and netrin-1 derived small peptides represent novel and robust therapeutic options for the treatment of PH, which can be readily translated into clinical practice in view of the advantageous, pharmaceutical applicability of small peptides.

2. Methods

2.1. Experimental design

All experiments were approved by the Institutional Animal Care and Usage Committee at the University of California, Los Angeles (UCLA). Male C57BL/6 mice of 9–12 weeks age (Charles River Laboratories, Wilmington, MA) were used for experimentation with a group as controls (n = 4–7). Another group of animals were kept under hypoxic condition (n = 5–8) and then harvested after 21 days for comparison. The hypoxic environment was maintained by mixed gas flow (normobaric 10% O2, in 5% CO2 balanced with 90% N2). The animals were fed and watered ad libitum, and cages were changed twice weekly. After the chamber was closed, the mixed gas was flushed to recover the hypoxic environment as quickly as possible. Animals were maintained at 20°C with a 12:12-h light-dark cycle. In hypoxic groups treated with netrin-1 or netrin-1 derived small peptides, age and body weight matched animals as for control and hypoxic groups were subcutaneously implanted of osmotic minipumps for continuous and stable release of netrin-1, or netrin-1 derived small peptides (V1, V2 or V3 peptide) at 15 ng/day (in delivery solution containing 152 mM NaCI, acetic acid at 1:100 for v/v, and distilled water) [31], and then harvested after 21 days. The netrin-1 derived small peptides V1-9aa (304–312 aa of human netrin-1; CDCRHNTAG), V2-10aa (368–377 aa of human netrin-1, CLNCRHNTAG), and V3-11aa (423–433 aa of human netrin-1, CPCKDGVTGIT) were synthesized by GenicBio Limited (Shanghai, China) [31].

2.2. Hemodynamic analyses

At the end of the treatment period, animals were anesthetized with intraperitoneal injection of pentobarbital at 60 mg/kg. The animals were intubated and connected to a respirator (95% O_2, 5% CO_2). Hemodynamic analyses were performed by an open chest method using the 1.4 F catheter (mikro-tip® catheter transducer; Model SPR-671, Millar Instruments, Houston, TX). The right ventricular systolic blood pressure (RVSP) and the mean pulmonary arterial pressure (mPAP) were recorded using a Power Lab data acquisition system (ADInstruments Inc., CO).

2.3. Tissue harvest, right heart assessment and histological examinations

After hemodynamic procedures, the mice were euthanized for resection of the heart and lung tissues, which were then weighed to assess the weight of the RV free wall, and the LV plus septum (LV + S). The ratio of the RV free wall to the free LV wall and the ventricular septum (RV/LV + S) was calculated to assess right heart hypertrophy by hypoxia treatment and its reversal by netrin-1 and netrin-1 derived small peptides. Middle region of the left lung tissues of all mice were submerged in ice-cold saline, perfused and subsequently fixed in 4% paraformaldehyde overnight followed by incubation for 24 h in 10% sucrose, and then embedded in paraffin for sectioning. Meanwhile, the superior lobe from the right lung were immersed in Tissue Plus® OCT compound (Thermo Fisher Scientific, Cat# 23730571, Houston, TX, USA) medium. Cryostat transverse cuts (5 μm) of lung OCT blocks were freshly prepared at -20°C for determination of ROS production and NO bioavailability using dihydroethidium (DHE) and 4-Amino-5-Methylamino-2',7'-Difluorofluorescein Diacetate (DAF-FM DA) fluorescent imaging respectively.

Specifically, lung paraffin sections of 5-μm thickness were stained with H&E. In each section, six randomly selected fields were examined with Nikon Eclipse Ti confocal microscope (Tokyo, Japan) for morphological analysis. Pulmonary arterioles with O.D. less than 200 μm were observed [36,37]. Percentage of medial wall thickness of pulmonary arterioles was measured using NIH Image J software. The medial thickness was categorically quantified for blood vessels with different diameters of 50–100 μm and 100–200 μm, and a separate figure was made for all blood vessels under the diameter of 200 μm. The pulmonary arterial medial wall thickness was calculated as % medial wall thickness = (wall thickness × 2/external diameter) × 100 [36,37]. For all histological analyses described here and below, at least 6–16 images were captured from each animal, and at least 6 individual fields of each image were analyzed.

2.4. Immunofluorecent assay and immunohistochemistry

Paraffin embedded lung sections of 5 μm thickness were dewaxed and rehydrated, followed by heat-mediated antigenic retrieval using a pH 6.0 citrate buffer for 20 min. Immunofluorescent assay and

immunohistochemistry examining smooth muscle alpha actin (SMA) and proliferating cell nuclear antigen (PCNA) expression were performed by incubating the lung sections with a rabbit antibody for SMA (1:200, Cat# ab5694, Abcam, Cambridge, MA, USA), or a mouse antibody for PCNA (1:50, Cat# ab29, Abcam, Cambridge, MA, USA). Next, the sections were incubated for 1 h with FITC-labelled goat anti-mouse IgG secondary antibody or Alexa Fluor goat anti-rabbit IgG secondary antibody and cover slipped. Fluorescent images were taken using a Nikon Eclipse Ti confocal microscope (Tokyo, Japan). Fluorescent intensity was quantified in six randomly selected fields in each section using the NIH Image J software. For 3,3-diaminobenzidine (DAB) staining, sections were incubated with secondary antibodies (1:200, Cat# PK-6102-mouse, NC9293436-rabbit, Vecta stain ABC kit, Vector labs, Burlingame, CA, USA) and stained using a DAB substrate according to the manufacturer's instructions (MilliporeSigma, Cat# D3939, St. Louis, MO, USA).

2.5. Masson's trichrome staining

Paraffin embedded lung tissue sections of 5-μm thickness were deparaffinized by sequential washes in xylene (2x), descending alcohol from 100% to 50%, and then distilled water. Then, the sections were subjected to Masson's Trichrome staining according to the manufacturer's instructions (MilliporeSigma, Cat# HT-15-1KT, St. Louis, MO, USA). Images were captured using Nikon Eclipse Ti confocal microscope (Tokyo, Japan). The perivascular and peribronchial collagen deposition in the lung was assessed by the percentage of fibrous tissue area in the visual field in Masson's Trichrome stained lung tissue sections. Blue is specific for collagen. Muscle fibers and cytoplasm were dyed red, and nuclei were dyed black. The images of were analyzed using NIH Image J software in six randomly selected microscopic fields for each section.

2.6. Determination of NO bioavailability

Lungs freshly isolated from mice were perfused slowly via the pulmonary artery to flush blood with Krebs HEPES buffer (KHB, pH 7.35), and immersed in Tissue Plus® OCT compound (Thermo Fisher Scientific, Cat# 23730571, Houston, TX, USA). Cryostat transverse cuts (5 μm) of lung sections were freshly prepared at -20°C. For determination of NO bioavailability using 4-Amino-5-Methylamino-2',7'-Difluorofluorescein Diacetate (DAF-FM DA) fluorescent probe as a recognized method detecting intracellular levels of NO [38], lung tissue sections were incubated with 20 μM DAF-FM DA (Thermo Fisher Scientific, Cat# D23844, Houston, TX, USA) for 20 min in dark at 37°C. After being washed for 3 times, the sections were coverslipped. The fluorescent images were captured using a Nikon Eclipse Ti confocal microscope (Tokyo, Japan) at excitation and emission wavelengths of 495 and 515 nm respectively, and six randomly selected fields in each section were quantified with the NIH Image J software.

2.7. Determination of reactive oxygen species (ROS) production

Briefly, the lungs freshly harvested from mice were perfused slowly from pulmonary artery to flush blood with Krebs HEPES buffer (KHB, pH 7.35), and immersed in Tissue Plus® OCT compound (Thermo Fisher Scientific, Cat# 23730571, Houston, TX, USA) medium. Cryostat transverse cuts (5 μm) of lung sections were freshly prepared at -20°C. Levels of ROS in mouse lungs were determined using dihydroethidium (DHE) fluorescent imaging as we previously published [19,39,40]. DHE stock solution was prepared by dissolving DHE (MilliporeSigma, Cat# D7008, St. Louis, MO, USA) in dimethylsulfoxide (DMSO) at a concentration of 2 mM. The stock solution was stored in the dark and diluted in KHB to a final concentration of 2 μM immediately prior to use. The tissue sections were washed with KHB and incubated in 2 μM DHE solution in a light-protected humidified chamber at 37°C for 30 min. Excessive DHE was rinsed off twice with KHB and the images were immediately captured with Nikon Eclipse Ti confocal microscope (Tokyo, Japan) at excitation and emission wavelengths of 520 and 610 nm, respectively. Fluorescent intensities of acquired digital images were quantified by NIH Image J software. Superoxide production and eNOS uncoupling activity were also determined using Electron Spin Resonance (ESR) as described below.

2.8. ESR determination of superoxide production and eNOS uncoupling activity

Electron spin resonance (ESR) is the gold standard for specific and quantitative detection of superoxide anion in biological systems. Briefly, freshly isolated lung tissues were homogenized on ice in lysis buffer containing 1:100 protease inhibitor cocktail, and centrifuged at 12,000 g for 10 min. Protein content of the supernatant was determined using a DC^{TM} protein assay kit (Bio-Rad, Cat# 500-0114 for reagent B, Cat# 500-0113 for reagent A, Cat# 400-0115 for reagent S, Hercules, CA, USA). eNOS uncoupling activity was determined from lung homogenates using ESR as we previously published [19,21,22,24,25,27–32,40–43]. Total superoxide production was calculated from the SOD-inhibitable fraction. For determination of eNOS uncoupling activity, superoxide production was measured in the presence or absence of NOS inhibitor L-NAME (10 μM, Cayman Chemical, Cat# 80587, Ann Arbor, MI, USA). When eNOS is healthy or coupled, L-NAME reduces NO production to result in less buffering effect of superoxide, hence an increase in superoxide detected. When NOS is "uncoupled", L-NAME treatment leads to reduction in superoxide production, which is derived from eNOS.

2.9. Statistical analysis

Statistical analyses of data were completed using Prism software. One-way ANOVA was used to compare means among different groups with a Newman-Keuls or Dunnett's Post-Hoc test. A statistical probability (p) value of < 0.05 was considered significant.

3. Results

3.1. Therapeutic effects of netrin-1 and netrin-1 derived small peptides on PH: attenuation of elevated mPAP and RVSP, and right ventricular hypertrophy

We examined potential protective effects of netrin-1 and netrin-1 derived small peptides against elevated pulmonary arterial pressure (mPAP) and right ventricular systolic pressure (RVSP) induced by hypoxia. Netrin-1 and netrin-1 derived small peptides substantially attenuated hypoxia induced increases in mPAP and RVSP in PH mice. As shown in Fig. 1A, mPAP in the hypoxia group was markedly increased to 42.96 ± 4.60 mmHg (n = 5), from 19.41 ± 1.28 mmHg in the normoxia group (n = 4). Netrin-1 protein itself reduced mPAP to 28.98 ± 2.11 mmHg (n = 5). Compared to the hypoxia group, levels of mPAP were substantially attenuated by treatment with netrin-1 derived small peptides to 23.83 ± 5.15 (V1 peptide, n = 4), 25.74 ± 3.79 mmHg (V2 peptide, n = 4), or 29.35 ± 3.64 mmHg (V3 peptide, n = 5).

Similarly in Fig. 1B, RVSP was significantly elevated in the hypoxia group at 43.77 ± 3.35 mmHg (n = 5), comparing to the normoxia group at 32.20 ± 1.88 mmHg (n = 4). Netrin-1 protein itself reduced RVSP to 32.19 ± 1.71 mmHg (n = 5). Intriguingly, increased RVSP by hypoxia was also near completely attenuated by treatment with netrin-1 derived small peptides to 31.50 ± 3.32 mmHg (V1 peptide, n = 4), 33.10 ± 1.04 mmHg (V2 peptide, n = 4), or 31.23 ± 1.77 mmHg (V3 peptide, n = 5).

Upon harvest after hypoxia exposure for 3 weeks, mouse hearts were freshly isolated and measured for weights of RV, and LV plus septum. As shown in Fig. 2, the RV/LV + S ratio was markedly increased in mice exposed to hypoxia (0.402 ± 0.015, n = 5), compared to the normoxia group (0.271 ± 0.013, n = 5). Compared to the hypoxia group, RV/LV

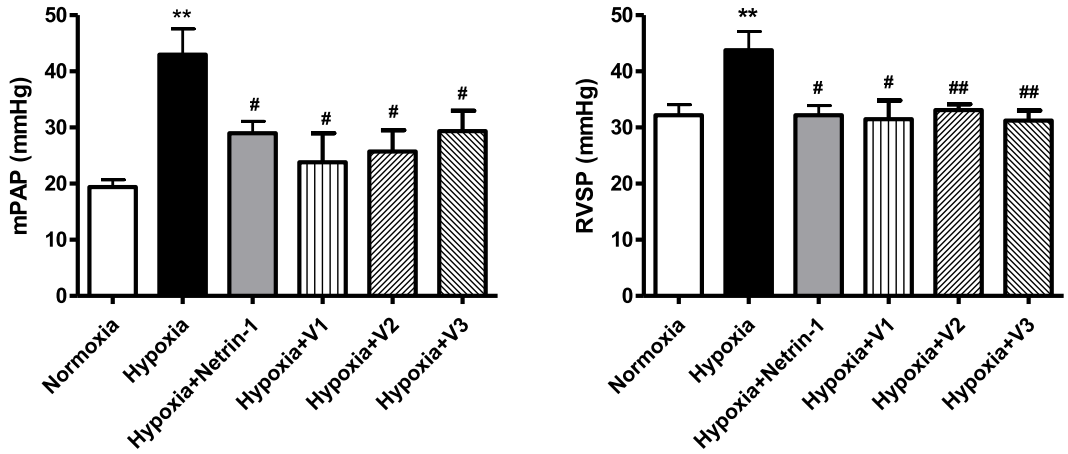

Fig. 1. Netrin-1 and netrin-1 derived small peptides attenuated elevations in mPAP and RVSP in pulmonary hypertensive mice. Pulmonary hypertension was induced in mice by exposure to normobaric hypoxia (10% O2) for three weeks. Osmotic pump was used to deliver netrin-1 or netrin-1 derived small peptides continuously. Hemodynamic analyses indicate that increased mPAP and RVSP in hypoxia induced pulmonary hypertensive mice were substantially attenuated by treatment with netrin-1 or netrin-1 derived small peptides V1, V2. or V3. Data are shown as Mean ± SEM. **p < 0.01 vs. Normoxia; #p < 0.05, ##, p < 0.01 vs. Hypoxia.

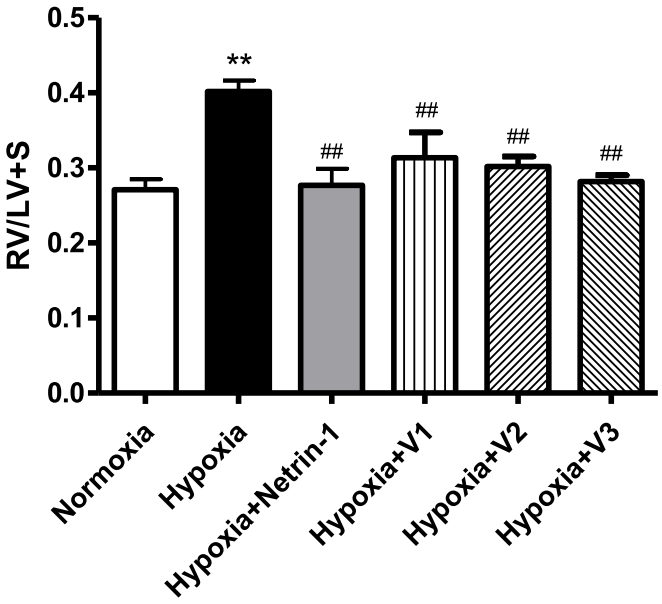

Fig. 2. Netrin-1 and netrin-1 derived small peptides attenuated right ventricular hypertrophy in pulmonary hypertensive mice. Pulmonary hypertension was induced in mice by exposure to normobaric hypoxia (10% O2) for three weeks. Osmotic pump was used to deliver netrin-1 or netrin-1 derived small peptides continuously. Right ventricle hypertrophy as indicated by increased RV/LV + S ratio in hypoxia induced pulmonary hypertensive mice was substantially attenuated by treatment with netrin-1 or netrin-1 derived small peptides V1, V2. or V3. Data are shown as Mean ± SEM. **p < 0.01 vs. Normoxia; ##p < 0.01 vs. Hypoxia.

+ S ratio was substantially attenuated by treatment with netrin-1 (0.277 ± 0.022, n = 5), V1 peptide (0.314 ± 0.033, n = 5), V2 peptide (0.302 ± 0.013, n = 5), or V3 peptide (0.282 ± 0.008, n = 5).

3.2. Therapeutic effects of netrin-1 and netrin-1 derived small peptides on PH: attenuation of pulmonary vascular remodeling

Pulmonary vascular remodeling was assessed by examination of medial thickness. The percentage medial thickness in blood vessels that have an external diameter less than 200 μm was significantly increased in the hypoxia group (n = 5) compared to the normoxia group (n = 5) (Fig. 3A & B). This elevation in percentage medial thickness in pulmonary blood vessels that have an external diameter less than 200 μm, was substantially decreased in animals treated with netrin-1 (n = 5), V1 peptide (n = 5), V2 peptide (n = 5), or V3 peptide (n = 5).

The percentage medial thickness in differently sized pulmonary arteries in the lung is shown in Fig. 3A & C. The percentage medial thickness in blood vessels that have an external diameter of 50–100 μm was significantly increased in the hypoxia group (n = 5) compared to the normoxia group (n = 3). Compared to the hypoxia group, percentage medial thickness in blood vessels that have an external diameter of 50–100 μm was markedly attenuated in animals treated with netrin-1 (n = 5), V1 peptide (n = 5), V2 peptide (n = 5), or V3 peptide (n = 5). The percentage medial thickness in blood vessels that have an external diameter of 100–200 μm was significantly increased in the hypoxia group (n = 5) compared to the normoxia group (n = 3), and this response was substantially attenuated by treatment with netrin-1 (n = 5), V1 peptide (n = 5), V2 peptide (n = 5), or V3 peptide (n = 5).

In order to examine potential lung vascular muscularization and cell proliferation, lung sections were stained with antibodies specific for smooth muscle actin (SMA) and proliferative cell nuclear antigen (PCNA). Both immunoflurecent and immunohistological analyses of lung tissues revealed vascular muscularization as evidenced by increased SMA-positive staining in hypoxia treated mouse pulmonary arterioles. The expression of SMA by immunofluorecent staining in the lung sections was markedly increased in the hypoxia group (n = 5) compared to the normoxia group (n = 4) (Fig. 4A & E). Compared to the hypoxia group, expression of SMA by immunofluorecent staining was substantially reduced by treatment with netrin-1 (n = 4), V1 peptide (n = 5), V2 peptide (n = 5), or V3 peptide (n = 5) (Fig. 4A & E). The expression of SMA by DAB staining in the lung sections was markedly increased in the hypoxia group (n = 4) compared to the control group (n = 5) (Fig. 4B & F). Compared to the hypoxia group, expression of SMA by DAB staining was substantially reduced by treatment with netrin-1 (n = 4), V1 peptide (n = 5), V2 peptide (n = 5), or V3 peptide (n = 5) (Fig. 4B & F).

Likewise, the expression of PCNA by immunofluorecent staining in the lung sections was markedly increased in the hypoxia group (n = 5) from the normoxia group (n = 4) (Fig. 4C & G). Compared to the hypoxia group, expression of PCNA by immunofluorecent staining was substantially reduced by treatment with netrin-1 (n = 4), V1 peptide (n = 5), V2 peptide (n = 5), or V3 peptide (n = 5) (Fig. 4C & G). In addition, expression of PCNA by DAB staining was markedly elevated in the

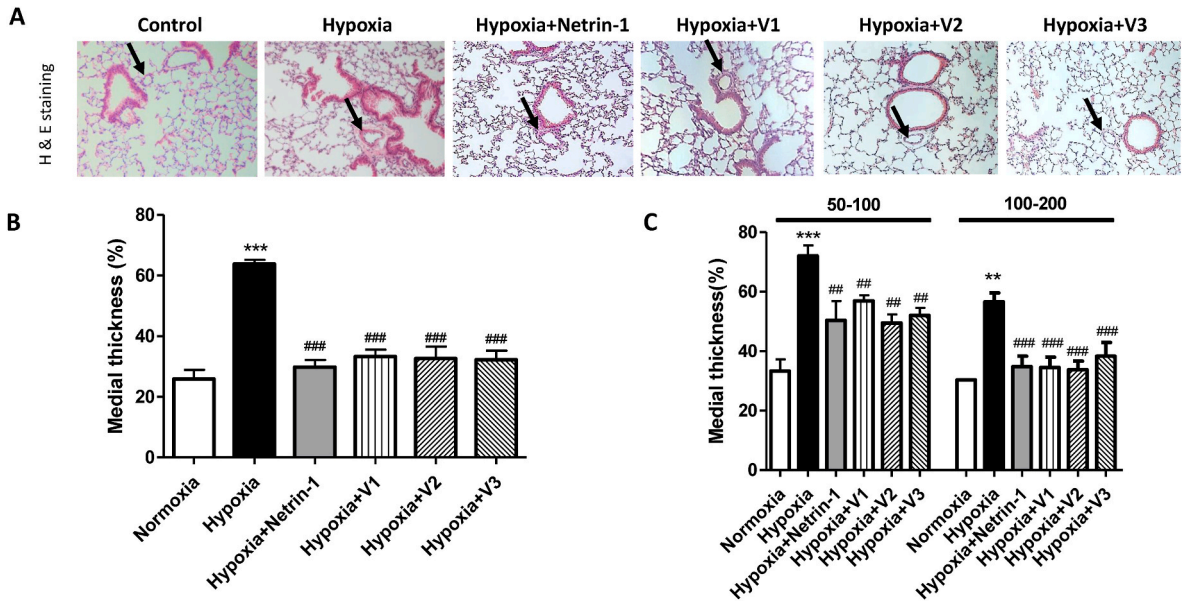

Fig. 3. Netrin-1 and netrin-1 derived small peptides alleviated vascular remodeling in pulmonary hypertensive mice. Pulmonary hypertension was induced in mice by exposure to normobaric hypoxia (10% O2) for three weeks. Osmotic pump was used to deliver netrin-1 or netrin-1 derived small peptides continuously. **(A)** Representative images of H&E staining (20X magnification) of lung tissue sections of various treatment groups. **(B)** Medial thickness of pulmonary arterioles (<200 μm in diameter) indicating increased medial thickness by hypoxia exposure, which was substantially alleviated by netrin-1 or netrin-1 derived peptides V1, V2 or V3. **(C)** Medial thickness in differently sized pulmonary arterioles indicating increased medial thickness by hypoxia exposure, which was substantially alleviated by netrin-1 or netrin-1 derived peptides V1, V2 or V3 in pulmonary arteries categorized by 50–100 and 100–200 μm in diameter. Data are shown as Mean ± SEM. **p < 0.01 or ***p < 0.001 vs. Normoxia; ##p < 0.01, ###p < 0.001 vs. Hypoxia.

hypoxia group (n = 5) compared to the normoxia group (n = 4) (Fig. 4D & H), confirming increased cell proliferation. Compared to the hypoxia group, expression of PCNA by DAB staining was markedly reduced by treatment with netrin-1 (n = 4), V1 peptide (n = 5), V2 peptide (n = 5), or V3 peptide (n = 5) (Fig. 4D & H).

In addition, peribronchial and perivascular collagen deposition as assessed by Mason's Trichrome staining was found markedly increased in lung tissue sections of hypoxia treated mice (n = 5) from the normoxia group (n = 5) (Fig. 5A & B). Compared to the hypoxia group, percentage fibrosis was significantly attenuated by treatment with netrin-1 (n = 5), V1 peptide (n = 5), V2 peptide (n = 5), or V3 peptide (n = 5) (Fig. 5A & B).

3.3. Therapeutic effects of netrin-1 and netrin-1 derived small peptides on PH: improvement in NO bioavailability and attenuation of ROS production

Endothelial nitric oxide (NO) bioavailability was assessed in mouse lungs *in situ* by fluorescent imaging using the NO-specific fluorescent probe DAF-FM DA. The image analysis of lung sections stained with DAF-FM DA showed decreased NO bioavailability in the hypoxia group (n = 5) compared to the normoxia group (n = 5) (Fig. 6A & C). Whereas, NO bioavailability was substantially or completely restored by treatment with netrin-1 (n = 5), V1 peptide (n = 5), V2 peptide (n = 5), or V3 peptide (n = 5) (Fig. 6A & C).

We next determined effects of hypoxia on ROS production in lung tissue sections. ROS production in lung tissue sections was determined using DHE fluorescent imaging. The image analysis of lung sections stained with DHE indicated increased ROS production in the hypoxia group (n = 7) compared to the normoxia group (n = 4) (Fig. 6B & D). Whereas, superoxide production was markedly attenuated by treatment with netrin-1 (n = 5), V1 peptide (n = 4), V2 peptide (n = 5), or V3 peptide (n = 5).

3.4. Therapeutic effects of Netrin-1 and peptides on PH: recoupling of eNOS

Electron spin resonance (ESR) was used as a gold standard to examine superoxide aninon production and eNOS uncoupling activity as we previously published [19,21,22,24,25,27–32,40–43]. Under normal conditions when eNOS is coupled, the addition of the NOS inhibitor L-NAME will increase the measured superoxide production, as eNOS is producing NO to scavenge superoxide; however, when eNOS is uncoupled and producing superoxide, its inhibition will lead to a decrease in measured superoxide. We examined whether eNOS was uncoupled in hyoxia exposed PH mice, and whether netrin-1 and netrin-1 derived small peptides can recouple eNOS. While superoxide production in mouse lungs by ESR determination was markedly increased by hypoxia exposure to 30.12 ± 3.12 μM/min/mg protein (n = 8) from the normoxia group (12.81 ± 2.84 μM/min/mg protein, n = 7), it was substantially attenuated by netrin-1 (19.09 ± 3.32 μM/min/mg protein, n = 5), V1 peptide (12.77 ± 3.16 μM/min/mg protein, n = 6), V2 peptide (14.78 ± 3.05 μM/min/mg protein, n = 6), or V3 peptide (8.52 ± 3.23 μM/min/mg protein, n = 5) (Fig. 7A). Of note, eNOS was markedly uncoupled as reflected by L-NAME inhibitable production of superoxide in Fig. 7B, which was reversed by treatment with netrin-1, V1 peptide, V2 peptide or V3 peptide (Fig. 7B). Taken together, these data indicate that via restoration of eNOS coupling activity to improve NO bioavailability and diminish oxidative stress, netrin-1 and netrin-1 derived small peptides are robustly effective in alleviating development of PH, which is characterized by attenuation of hemodynamic changes of elevated mPAP and RVSP, right heart hypertrophy, as well as features of vascular remodeling of increased medial thickness, muscularization, proliferation and fibrosis.

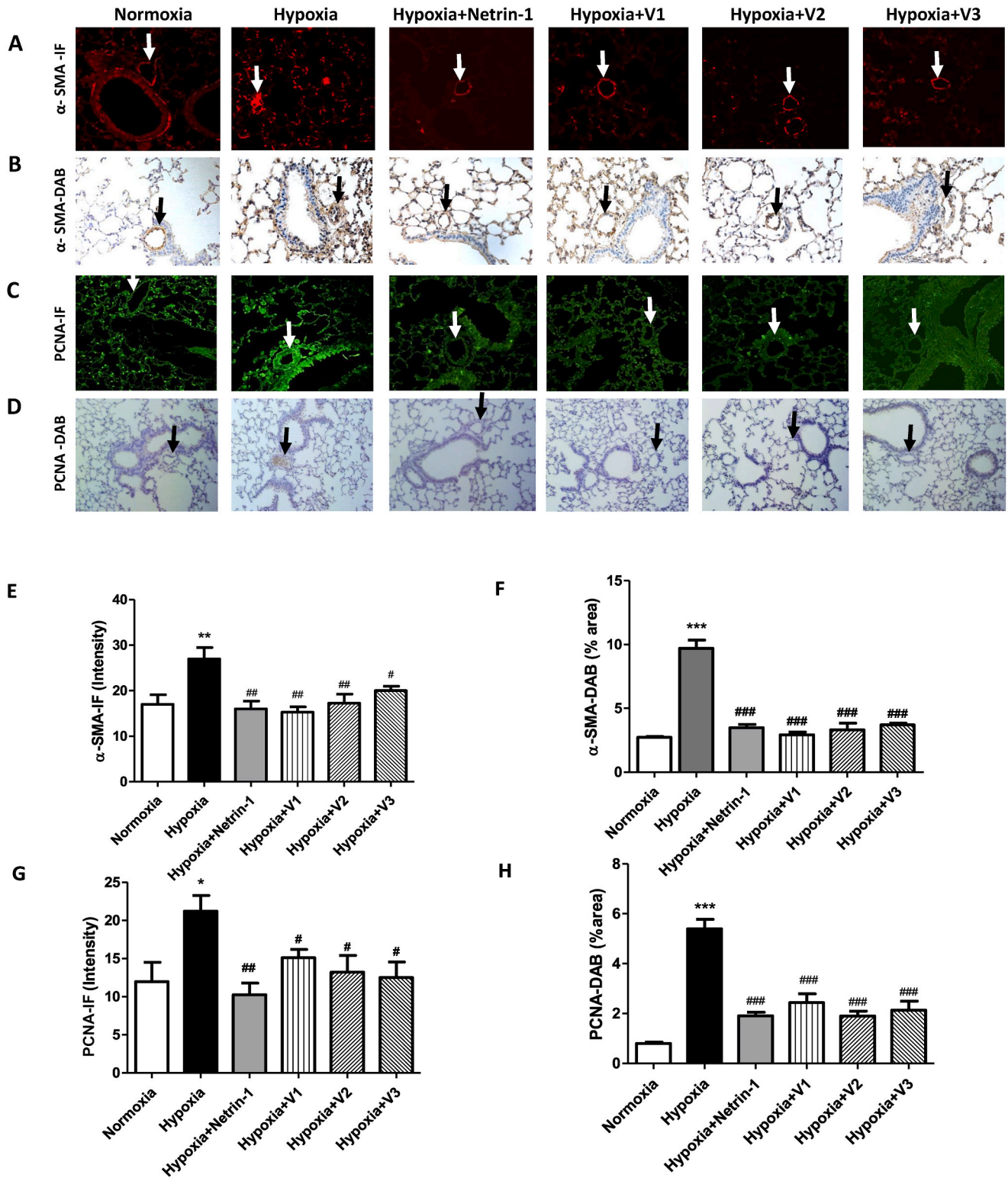

Fig. 4. Netrin-1 and netrin-1 derived small peptides attenuated muscularization and cell proliferation of blood vessels in pulmonary hypertensive mice. Pulmonary hypertension was induced in mice by exposure to normobaric hypoxia (10% O2) for three weeks. Osmotic pump was used to deliver netrin-1 or netrin-1 derived small peptides continuously. **(A, E)** Representative images and quantitative data of smooth muscle actin (SMA) expression by immunoflurescent staining indicating increased SMA expression by hypoxia exposure, which was substantilly attenuated by netrin-1 or netrin-1 derived peptides V1, V2 or V3. **(B, F)** Representative images and quantitative data of SMA expression by immunohistochemical staining using DAB substrate indicating increased SMA expression by hypoxia exposure, which was substantially attenuated by netrin-1 or netrin-1 derived peptides V1, V2 or V3. **(C, G)** Representative images and quantitative data of proliferative cell nuclear antigen (PCNA) expression by immunoflurescent staining indicating increased PCNA expression by hypoxia exposure, which was markedly attenuated by netrin-1 or netrin-1 derived peptides V1, V2 or V3. **D, H)** Representative images and quantitative data of PCNA expression by immunohistochemical staining using DAB substrate indicating increased PCNA expression by hypoxia exposure, which was markedly attenuated by netrin-1 or netrin-1 derived peptides V1, V2 or V3. Data are shown as Mean ± SEM. *p < 0.05, **p < 0.01 or ***p < 0.001 vs. Normoxia; #p < 0.05, ##p < 0.01, ###p < 0.001 vs. Hypoxia.

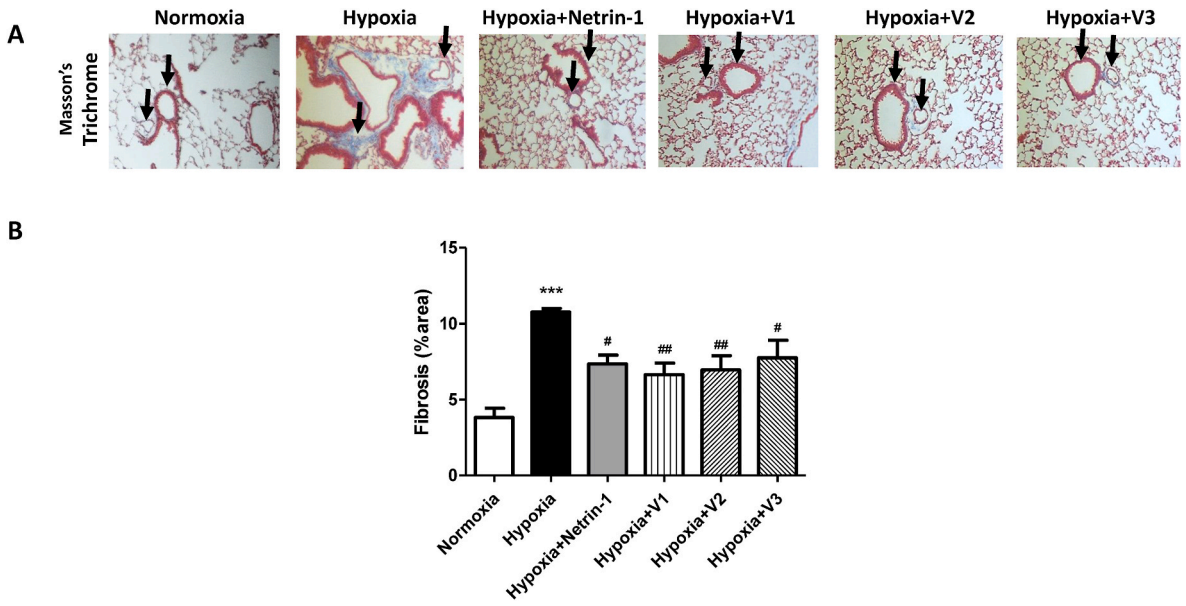

Fig. 5. Netrin-1 and netrin-1 derived small peptides alleviated fibrosis in pulmonary hypertensive mice. Pulmonary hypertension was induced in mice by exposure to normobaric hypoxia (10% O2) for three weeks. Osmotic pump was used to deliver netrin-1 or netrin-1 derived small peptides continuously. **(A, B)** Representative images and grouped data of Masson's Trichrome staining indicating increased collagen deposition (blue; x20 magnification) in peribronchial and perivascular areas of lung sections in hypoxia exposed mice, which was markedly alleviated by netrin-1 or netrin-1 derived small peptides V1, V2 or V3. Data are shown as Mean ± SEM. ***$p < 0.001$ vs. Normoxia; #$p < 0.05$, ##$p < 0.01$ vs. Hypoxia.

4. Discussion

The most significant finding of the present study is that netrin-1 and netrin-1 derived small peptides can serve as novel and robust therapeutic regimes for the devastating cardiorespiratory disease of pulmonary hypertension (PH). Our innovative observations demonstrate that: 1) Hemodynamic changes of elevated mPAP and RVSP, and right heart hypertrophy, pathophysiological hallmarks of PH, were substantially alleviated by netrin-1 and netrin-1 derived small peptides of V1, V2 or V3 in a hypoxia induced classical model of PH in mice; 2) Vascular remodeling of pulmonary arterioles featured by increased medial thickness, muscularization, proliferation and fibrosis, markedly induced by hypoxia in mice as important pathophysiological processes underlying development of PH, was substantially abrogated by netrin-1 or netrin-1 derived small peptides of V1, V2 or V3; 3) Treatment of hypoxia exposed mice with netrin-1 or netrin-1 derived small peptides of V1, V2 or V3 substantially attenuated superoxide production/oxidative stress and reversed eNOS uncoupling status, while improving NO bioavailability to result in reduced vasoconstriction and alleviated vascular remodeling to abrogate development of PH. These findings no double establish novel therapeutic efficacies of netrin-1 and netrin-1 derived small peptides in the treatment of PH, especially with small peptides being pharmaceutically convenient for clinical application.

Despite of decades long efforts, treatments to effectively stop or regress development of PH have been lacking [8,44]. The current therapies mostly target the early phase of the disease to improve vasodilation, while the later remodeling phase of the disease not altered. Nonetheless, PH is a severe cardiorespiratory disorder with patients die young, consequent to limited therapeutic options and lack of donor lungs when transplantation becomes the only option to treat end stage disease. Therefore, it is critically important to develop novel and effective therapeutics. Medications targeting NO pathway alone have been used clinically, such as inhaled NO, PDE-5 inhibitors (sildenafil and tadalafil) and sGC simulator (riociguat), which have been shown to be effective in relieving symptoms of PH [7,8,10]. It is not enough to treat more advanced disease and here we propose that treatments targeting NO while attenuating oxidative stress, would be more effective in allelviating PH, especially for the remodeling phase that has been shown to be mediated by oxidative stress [20,26,33]. Indeed, our data in the present study indicate that netrin-1 and netrin-1 derived small peptides are robustly effective in attenuting lung superoxide production and restoring eNOS coupling activity in hypoxia treated mice, resulting in an improved redox balance of both decrease in ROS and increase in NO. These responses represent major mechanisms responsible for the robust therapeutic efficacies of netrin-1 and netrin-1 derived small peptides. Of note, netrin-1 and its derived small peptides can activate netrin-1 receptor DCC to lead to production of NO from coupled eNOS, as well as attenuation of oxidative stress through inhibition of NOX4/-eNOS uncoupling axis during cardiac ischemia reperfusion injury [23,27–29,31,34,35]. Indeed, activation of NOX4 has been implicated in hypoxia induced development of PH [45,46].

It is important to note that all of the pathophysiological and molecular features of PH in hypoxia exposed mice were substantially alleviated by netrin-1 and netrin-1 derived small peptides. These include hemodynamic parameters determined by the gold standard of right heart catheterization technology. Hypoxia induced increases in mPAP and RVSP, as well as right heart hypertrophy, were all substantially attenuated by osmotic minipump mediated continuous infusion into mice of netrin-1 and netrin-1 derived small peptides. The typical vascular remodeling responses of increased medial thickness, muscularization, proliferation and fibrosis, were also substantially abrogated by netrin-1 and its derived small peptides. In addition, ROS and superoxide anion production defined by both fluorescent imaging and ESR analyses, markedly increased in hypoxia exposed mice, was also substantially alleviated by netrin-1 and netrin-1 derived small peptides. These protective effects on PH of netrin-1 and its derived small peptides are attributed to recoupling of eNOS to result in restoration of eNOS function/improved NO bioavailability and abrogation of oxidative stress. These mechanistic insights identified share similarity with our previous findings regarding cardioprotective effects of netrin-1 and netrin-1 derived small peptides [23,27–29,31,34,35].

In conclusion, our findings for the first time establish novel and robust therapeutic efficacies of netrin-1 and netrin-1 derived small peptides on PH, with the full scope of pathophysiological and

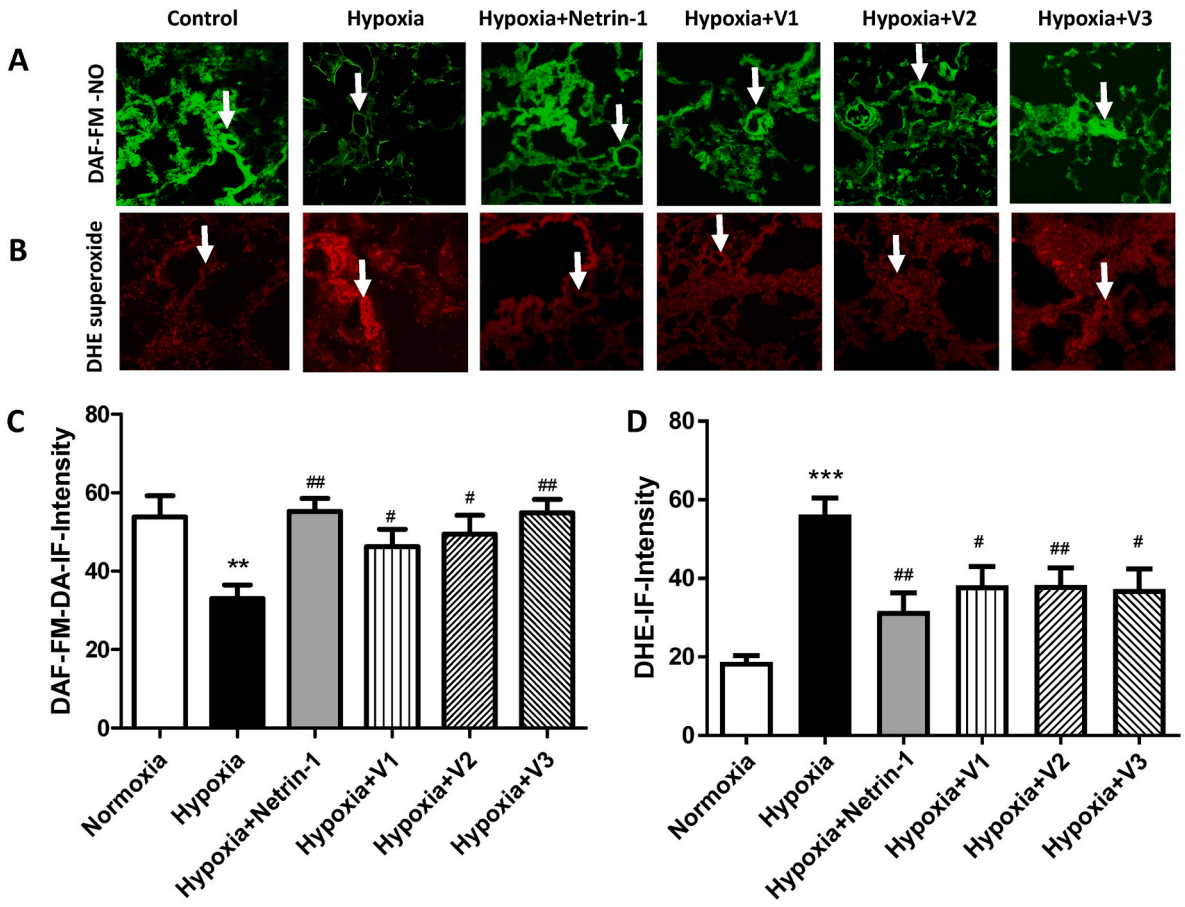

Fig. 6. Netrin-1 and netrin-1 derived small peptides improved NO bioavailability while attenuating ROS production in pulmonary hypertensive mice. Pulmonary hypertension was induced in mice by exposure to normobaric hypoxia (10% O2) for three weeks. Osmotic pump was used to deliver netrin-1 or netrin-1 derived small peptides continuously. **(A, C)** Representative images and quantitative data of NO bioavailability by DAF-FM fluorescent imaging indicating NO deficiency in hypoxia exposed mice, which was substantially improved by netrin-1 or netrin-1 derived small peptides V1, V2 or V3. n = 5–7. **(B, D)** Representative images and quantitative data of ROS production by DHE fluorescent imaging indicating increased ROS production in hypoxia exposed mice, which was markedly attenuated by netrin-1 or netrin-1 derived small peptides V1, V2 or V3. Data are shown as Mean ± SEM. **p < 0.01 or ***p < 0.001 vs. Normoxia; #p < 0.05 or ##p < 0.01 vs. Hypoxia.

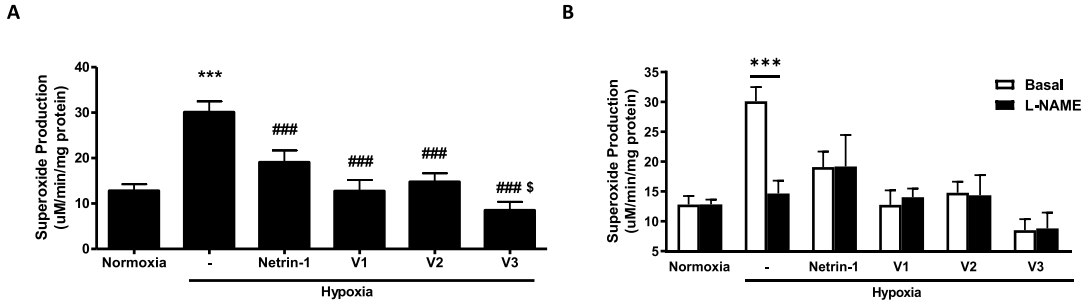

Fig. 7. Netrin-1 and netrin-1 derived small peptides abrogated superoxide production and eNOS uncoupling activity in pulmonary hypertensive mice. Pulmonary hypertension was induced in mice by exposure to normobaric hypoxia (10% O2) for three weeks. Osmotic pump was used to deliver netrin-1 or netrin-1 derived small peptides continuously. Lung tissues were used to measure total superoxide production and eNOS uncoupling activity using electron spin resonance (ESR) as we previously published. **(A)** Grouped data of total superoxide production determined by ESR indicating increased superoxide production in hypoxia exposed mice, which was substantially attenuated by netrin-1 and netrin-1 derived small peptides V1, V2 or V3. ***p<0.001 vs. Normoxia, ###p<0.001 vs. Hypoxia, $p<0.05 vs. Hypoxia plus Netrin-1 by One-Way ANOVA. **(B)** Grouped data of superoxide production in the presence or absence of L-NAME for assessment of eNOS uncoupling activity indicating uncoupling of eNOS (reflected by L-NAME sensitive superoxide production) in hypoxic pulmonary hypertensive mice, which was reversed by netrin-1 or netrin-1 derived small peptides V1, V2 or V3. ***p<0.001 by *t*-test.

molecular phenotypes substantially alleviated. These effects are attributed to recoupling of eNOS/restoration of eNOS function to abrogate oxidative stress while improving NO bioavailability. In view of the pharmaceutical advantages of peptide drugs, these observations would no doubt facilitate rapid translation of benchtop discoveries to clinical practice for the treatment of PH, for which effective therapies are urgently in need to better manage the devastating and lethal cardiorespiratory disorder.

Acknowledgement

The study was supported by National Institute of Health (NIH) National Heart Lung and Blood Institute (NHLBI) awards HL077440 (H.C.), HL088975 (H.C.), HL142951 (H.C.), HL154754 (H.C., A.M.) and HL162407 (H.C., J.G.).

Appendix A. Supplementary data

Supplementary data to this article can be found online at https://doi.org/10.1016/j.redox.2022.102348.

References

[1] D.B. Badesch, H.C. Champion, M.A. Gomez Sanchez, M.M. Hoeper, J.E. Loyd, A. Manes, M. McGoon, R. Naeije, H. Olschewski, R.J. Oudiz, A. Torbicki, Diagnosis and assessment of pulmonary arterial hypertension, J. Am. Coll. Cardiol. 54 (2009) S55–S66.
[2] A.L. Firth, J. Mandel, J.X. Yuan, Idiopathic pulmonary arterial hypertension, Dis Model Mech 3 (2010) 268–273.
[3] S.Y. Chan, J. Loscalzo, Pulmonary vascular disease related to hemodynamic stress in the pulmonary circulation, Compr. Physiol. 1 (2011) 123–139.
[4] J.Y. Luo, Y. Zhang, L. Wang, Y. Huang, Regulators and effectors of bone morphogenetic protein signalling in the cardiovascular system, J. Physiol. 593 (2015) 2995–3011.
[5] Z. Dai, M.M. Zhu, Y. Peng, N. Machireddy, C.E. Evans, R. Machado, X. Zhang, Y. Y. Zhao, Therapeutic targeting of vascular remodeling and right heart failure in pulmonary arterial hypertension with a HIF-2α inhibitor, Am. J. Respir. Crit. Care Med. 198 (2018) 1423–1434.
[6] D. Yi, B. Liu, T. Wang, Q. Liao, M.M. Zhu, Y.Y. Zhao, Z. Dai, Endothelial autocrine signaling through CXCL12/CXCR4/FoxM1 Axis contributes to severe pulmonary arterial hypertension, Int. J. Mol. Sci. (2021) 22.
[7] E. Loh, J.S. Stamler, J.M. Hare, J. Loscalzo, W.S. Colucci, Cardiovascular effects of inhaled nitric oxide in patients with left ventricular dysfunction, Circulation 90 (1994) 2780–2785.
[8] J.A. Leopold, S.M. Kawut, M.A. Aldred, S.L. Archer, R.L. Benza, M.R. Bristow, E. L. Brittain, N. Chesler, F.S. DeMan, S.C. Erzurum, M.T. Gladwin, P.M. Hassoun, A. R. Hemnes, T. Lahm, J.A.C. Lima, J. Loscalzo, B.A. Maron, L.M. Rosa, J. H. Newman, S. Redline, S. Rich, F. Rischard, L. Sugeng, W.H.W. Tang, R.J. Tedford, E.J. Tsai, C.E. Ventetuolo, Y. Zhou, N.R. Aggarwal, L. Xiao, Diagnosis and Treatment of Right Heart Failure in Pulmonary Vascular Diseases: A National Heart, Lung, and Blood Institute Workshop, Circ Heart Fail, 2021, p. 14.
[9] A. Raiesdana, J. Loscalzo, Pulmonary arterial hypertension, Ann. Med. 38 (2006) 95–110.
[10] M. Humbert, H.A. Ghofrani, The molecular targets of approved treatments for pulmonary arterial hypertension, Thorax 71 (2016) 73–83.
[11] T. Hansen, K.K. Galougahi, D. Celermajer, N. Rasko, O. Tang, K.J. Bubb, G. Figtree, Oxidative and nitrosative signalling in pulmonary arterial hypertension - implications for development of novel therapies, Pharmacol. Ther. 165 (2016) 50–62.
[12] N. Ghasemzadeh, R.S. Patel, D.J. Eapen, E. Veledar, H. Al Kassem, P. Manocha, M. Khayata, A.M. Zafari, L. Sperling, D.P. Jones, A.A. Quyyumi, Oxidative stress is associated with increased pulmonary artery systolic pressure in humans, Hypertension 63 (2014) 1270–1275.
[13] A. Smukowska-Gorynia, P. Rzymski, J. Marcinkowska, B. Poniedziałek, A. Komosa, A. Cieslewicz, S. Slawek-Szmyt, M. Janus, A. Araszkiewicz, S. Jankiewicz, I. Tomaszewska-Krajniak, T. Mularek-Kubzdela, Prognostic value of oxidative stress markers in patients with pulmonary arterial or chronic thromboembolic pulmonary hypertension, Oxid. Med. Cell. Longev. (2019), 3795320..
[14] H. Cai, D.G. Harrison, Endothelial dysfunction in cardiovascular diseases: the role of oxidant stress, Circ. Res. 87 (2000) 840–844.
[15] H. Cai, K.K. Griendling, D.G. Harrison, The vascular NAD(P)H oxidases as therapeutic targets in cardiovascular diseases, Trends Pharmacol. Sci. 24 (2003) 471–478.
[16] D. Harrison, K.K. Griendling, U. Landmesser, B. Hornig, H. Drexler, Role of oxidative stress in atherosclerosis, Am. J. Cardiol. 91 (2003) 7A–11A.
[17] H. Cai, Hydrogen peroxide regulation of endothelial function: mechanisms, consequences and origins, Cardiovasc. Res. 68 (2005) 26–36.
[18] H. Cai, NAD(P)H oxidase-dependent self-propagation of hydrogen peroxide and vascular disease, Circ. Res. 96 (2005) 818–822.
[19] J.H. Oak, H. Cai, Attenuation of angiotensin II signaling recouples eNOS and inhibits nonendothelial NOX activity in diabetic mice, Diabetes 56 (2007) 118–126.
[20] A.L. Firth, J.X. Yuan, Bringing down the ROS: a new therapeutic approach for PPHN, Am. J. Physiol. Lung Cell Mol. Physiol. 295 (2008) L976–L978.
[21] J.H. Oak, J.Y. Youn, H. Cai, Aminoguanidine inhibits aortic hydrogen peroxide production, VSMC NOX activity and hypercontractility in diabetic mice, Cardiovasc. Diabetol. 8 (2009) 65.
[22] L. Gao, K. Chalupsky, E. Stefani, H. Cai, Mechanistic insights into folic acid-dependent vascular protection: dihydrofolate reductase (DHFR)-mediated reduction in oxidant stress in endothelial cells and angiotensin II-infused mice. A Novel HPLC-based Fluorescent Assay for DHFR Activity, J. Mol. Cell. Cardiol. 47 (2009) 752–760.
[23] J. Zhang, H. Cai, Netrin-1 prevents ischemia/reperfusion-induced myocardial infarction via a DCC/ERK1/2/eNOS(s1177)/NO/DCC feed-forward mechanism, J. Mol. Cell. Cardiol. 48 (2010) 1060–1070.
[24] L. Gao, K.L. Siu, K. Chalupsky, A. Nguyen, P. Chen, N.L. Weintraub, Z. Galis, H. Cai, Role of uncoupled endothelial nitric oxide synthase in abdominal aortic aneurysm formation: treatment with folic acid, Hypertension 59 (2012) 158–166.
[25] J.Y. Youn, L. Gao, H. Cai, The p47phox- and NADPH oxidase organiser 1 (NOXO1)-dependent activation of NADPH oxidase 1 (NOX1) mediates endothelial nitric oxide synthase (eNOS) uncoupling and endothelial dysfunction in a streptozotocin-induced murine model of diabetes, Diabetologia 55 (2012) 2069–2079. Epub 2012 May 2.
[26] S. Aggarwal, C.M. Gross, S. Sharma, J.R. Fineman, S.M. Black, Reactive oxygen species in pulmonary vascular remodeling, Compr. Physiol. 3 (2013) 1011–1034.
[27] K.L. Siu, C. Lotz, P. Ping, H. Cai, Netrin-1 abrogates ischemia/reperfusion-induced cardiac mitochondrial dysfunction via nitric oxide-dependent attenuation of NOX4 activation and recoupling of NOS, J. Mol. Cell. Cardiol. 78 (2014) 174–185.
[28] J.O. Bouhidel, P. Wang, K.L. Siu, H. Li, J.Y. Youn, H. Cai, Netrin-1 improves post-injury cardiac function in vivo via DCC/NO-dependent preservation of mitochondrial integrity, while attenuating autophagy, Biochim. Biophys. Acta 1852 (2015) 277–289.
[29] Q. Li, P. Wang, K. Ye, H. Cai, Central role of SIAH inhibition in DCC-dependent cardioprotection provoked by netrin-1/NO, Proc. Natl. Acad. Sci. U. S. A. 112 (2015) 899–904.
[30] Q. Li, J.Y. Youn, H. Cai, Mechanisms and consequences of endothelial nitric oxide synthase dysfunction in hypertension, J. Hypertens. 33 (2015) 1128–1136.
[31] Q. Li, H. Cai, Induction of cardioprotection by small netrin-1-derived peptides, Am. J. Physiol. Cell Physiol. 309 (2015) C100–C106.
[32] Y. Zhang, P. Murugesan, K. Huang, H. Cai, NADPH oxidases and oxidase crosstalk in cardiovascular diseases: novel therapeutic targets, Nat. Rev. Cardiol. 17 (2020) 170–194.
[33] R. Faraj, D. Paine, S.M. Black, T. Wang, Anti-inflammatory effects of statins in lung vascular pathology: from basic science to clinical trials, Adv. Exp. Med. Biol. 1303 (2021) 33–56.
[34] A. Nguyen, H. Cai, Netrin-1 induces angiogenesis via a DCC-dependent ERK1/2-eNOS feed-forward mechanism, Proc. Natl. Acad. Sci. U. S. A. 103 (2006) 6530–6535.
[35] N.M. Liu, K.L. Siu, J.Y. Youn, H. Cai, Attenuation of neointimal formation with netrin-1 and netrin-1 preconditioned endothelial progenitor cells, J. Mol. Med. (Berl.) 95 (2017) 335–348.
[36] J.C. Wanstall, A. Gambino, T.K. Jeffery, M.M. Cahill, D. Bellomo, N.K. Hayward, G. F. Kay, Vascular endothelial growth factor-B-deficient mice show impaired development of hypoxic pulmonary hypertension, Cardiovasc. Res. 55 (2002) 361–368.
[37] S. Mizuno, H.J. Bogaard, D. Kraskauskas, A. Alhussaini, J. Gomez-Arroyo, N. F. Voelkel, T. Ishizaki, p53 Gene deficiency promotes hypoxia-induced pulmonary hypertension and vascular remodeling in mice, Am. J. Physiol. Lung Cell Mol. Physiol. 300 (2011) L753–L761.
[38] Y. Yu, Y. Xiong, J.P. Montani, Z. Yang, X.F. Ming, En face detection of nitric oxide and superoxide in endothelial layer of intact arteries, J Vis Exp (2016), 53718.
[39] J.Y. Youn, A. Nguyen, H. Cai, Inhibition of XO or NOX attenuates diethylstilbestrol-induced endothelial nitric oxide deficiency without affecting its effects on LNCaP cell invasion and apoptosis, Clin. Sci. (Lond.) 123 (2012) 509–518.
[40] K. Huang, T. Narumi, Y. Zhang, Q. Li, P. Murugesan, Y. Wu, N.M. Liu, H. Cai, Targeting MicroRNA-192-5p, a downstream effector of NOXs (NADPH oxidases), reverses endothelial DHFR (dihydrofolate reductase) deficiency to attenuate abdominal aortic aneurysm formation, Hypertension 78 (2021) 282–293.
[41] K. Chalupsky, H. Cai, Endothelial dihydrofolate reductase: critical for nitric oxide bioavailability and role in angiotensin II uncoupling of endothelial nitric oxide synthase, Proc. Natl. Acad. Sci. U. S. A. 102 (2005) 9056–9061. Epub 2005 Jun 7.
[42] K. Huang, Y. Wang, K.L. Siu, Y. Zhang, H. Cai, Targeting feed-forward signaling of TGFβ/NOX4/DHFR/eNOS uncoupling/TGFβ axis with anti-TGFβ and folic acid

attenuates formation of aortic aneurysms: novel mechanisms and therapeutics, Redox Biol. 38 (2021), 101757.
[43] Z. Guo, Y. Zhang, C. Liu, J.Y. Youn, H. Cai, Toll-like receptor 2 (TLR2) knockout abrogates diabetic and obese phenotypes while restoring endothelial function via inhibition of NOX1, Diabetes 70 (2021) 2107–2119.
[44] S.A. Mandras, H.S. Mehta, A. Vaidya, Pulmonary hypertension: a brief guide for clinicians, Mayo Clin. Proc. 95 (2020) 1978–1988.
[45] D.E. Green, T.C. Murphy, B.Y. Kang, J.M. Kleinhenz, C. Szyndralewiez, P. Page, R. L. Sutliff, C.M. Hart, The Nox4 inhibitor GKT137831 attenuates hypoxia-induced pulmonary vascular cell proliferation, Am. J. Respir. Cell Mol. Biol. 47 (2012) 718–726.
[46] S. Wedgwood, S. Lakshminrusimha, L. Czech, P.T. Schumacker, R.H. Steinhorn, Increased p22(phox)/Nox4 expression is involved in remodeling through hydrogen peroxide signaling in experimental persistent pulmonary hypertension of the newborn, Antioxidants Redox Signal. 18 (2013) 1765–1776.